2017

Archelosaurian Color Vision, Parietal Eye Loss, and the Crocodylian Nocturnal Bottleneck

Christopher A. Emerling
cemerlin@whittier.edu

Recommended Citation

Emerling, C. A. (2017). Archelosaurian color vision, parietal eye loss, and the crocodylian nocturnal bottleneck. Molecular biology and evolution, 34(3), 666-676. https://doi.org/10.1093/molbev/msw265

Archelosaurian Color Vision, Parietal Eye Loss, and the Crocodylian Nocturnal Bottleneck

Christopher A. Emerling*[,1]
[1]Museum of Vertebrate Zoology, University of California Berkeley, Berkeley, CA
*Corresponding author: E-mail: caemerling@berkeley.edu.
Associate editor: Nicolas Vidal

Abstract

Vertebrate color vision has evolved partly through the modification of five ancestral visual opsin proteins via gene duplication, loss, and shifts in spectral sensitivity. While many vertebrates, particularly mammals, birds, and fishes, have had their visual opsin repertoires studied in great detail, testudines (turtles) and crocodylians have largely been neglected. Here I examine the genomic basis for color vision in four species of turtles and four species of crocodylians, and demonstrate that while turtles appear to vary in their number of visual opsins, crocodylians experienced a reduction in their color discrimination capacity after their divergence from Aves. Based on the opsin sequences present in their genomes and previous measurements of crocodylian cones, I provide evidence that crocodylians have co-opted the rod opsin (RH1) for cone function. This suggests that some crocodylians might have reinvented trichromatic color vision in a novel way, analogous to several primate lineages. The loss of visual opsins in crocodylians paralleled the loss of various anatomical features associated with photoreception, attributed to a "nocturnal bottleneck" similar to that hypothesized for Mesozoic mammals. I further queried crocodylian genomes for nonvisual opsins and genes associated with protection from ultraviolet light, and found evidence for gene inactivation or loss for several of these genes. Two genes, encoding parietopsin and parapinopsin, were additionally inactivated in birds and turtles, likely co-occurring with the loss of the parietal eye in these lineages.

Key words: **opsins, color vision, Crocodylia, Testudinata, parietal eye, nocturnal bottleneck.**

Introduction

Vision is a critical sensory modality for most vertebrates, being important for foraging, predator avoidance, conspecific recognition, and migration. While aspects of the molecular basis for vision have been elucidated in many groups of vertebrates (Davies et al. 2012), Crocodylia and Testudinata (turtles) have largely been neglected. The currently species poor Crocodylia (24 extant spp.) originated ~93 Ma (Oaks 2011) and is represented today by Alligatoridae, Crocodylidae, and Gavialidae. Despite being the sole descendants of a Triassic radiation of pseudosuchian archosaurs (Nesbitt 2011) and the closest living relatives of the frequently colorful and highly visual Aves, little is known about how their visual system has evolved.

An important question about crocodylian vision stems from Walls (1942) seminal work on comparative ocular anatomy in vertebrates. In it, he states that crocodylian eyes "bear the stigmata of a long-continued nocturnality" (p. 613), including a rod-dominated retina, retinal regions containing cones that are "made as rod-like as possible" (Walls 1942, p. 616), a light collecting tapetum lucidum, and the absence of cone oil droplets, sclerotic rings (Nesbitt et al. 2013) and an annular pad of the lens (Walls 1942). Nagloo et al. (2016) also described a relatively large lens in crocodiles, typically associated with nocturnality, and retinal ganglion cell densities comparable to those of nocturnal squamates. Notably, many of these features are shared with mammals, which are thought to have undergone a long period of dim-light adaptation during the Mesozoic, termed a "nocturnal bottleneck" (Walls 1942; Gerkema et al. 2013). Recent studies have revealed that mammals reduced their genomic complement of light-associated genes, including both visual and nonvisual opsins (Gerkema et al. 2013) and enzymes that mitigate ultraviolet photo-oxidative damage (Kato et al. 1994; Osborn et al. 2015). If crocodylians did indeed experience a nocturnal bottleneck, a similar degree of light-associated gene inactivation and deletion should be reflected in crocodylian genomes.

Testudinata is represented today by >300 species distributed across 14 families, with a fossil record that dates back to the Triassic (Joyce and Gauthier 2004; Li et al. 2008). A combination of recent genomic and fossil discoveries suggests that turtles are diapsid amniotes (Chiari et al. 2012; Schoch and Sues 2015), but the ecological origins of turtles are contentious: the very early stem testudine *Odontochelys semitestacea* was discovered in marine deposits (Li et al. 2008) and phylogeneticists frequently recover turtles as sister to the marine sauropterygians (Lee 2013), but various other stem turtles show evidence of terrestrial adaptations (Joyce and Gauthier 2004; Scheyer and Sander 2007; Anquetin 2011). Regardless of the precise timing of aquatic adaptation, the phylogenetic distribution of extant testudines unambiguously reconstructs the ancestor of crown turtles as a freshwater inhabitant (Joyce and Gauthier 2004). This, coupled with shifts to marine habitats (e.g., Chelonoidea), suggests that

turtles may have experienced molecular adaptations to their visual system, similar to what has occurred in marine mammals (Levenson et al. 2006; Meredith et al. 2013).

To test these hypotheses, I searched the genomes of four crocodylians and four testudines for genes encoding both visual and nonvisual photoreceptive opsins and genes encoding enzymes that protect against UV-light photo-oxidative damage. I provide evidence that turtles ancestrally possessed the capacity for tetrachromatic (four color channels) color vision, with trionychid turtles losing some short wavelength visual opsins, whereas stem crocodylians underwent a reduction in their genes associated with light-sensitivity, including color vision, thus consistent with the hypothesis of passing through a nocturnal bottleneck early in their history. Additionally, the presence of parietal eye-related pseudogenes in crocodylians, birds, and testudines correlates with the loss of the parietal (third) eye early in their respective histories.

Results and Discussion

I examined publically available genomes for species representing the three crocodylian families, Alligatoridae (*Alligator mississippiensis* [American alligator; 156× coverage], *Alligator sinensis* [Chinese alligator; 109×]), Crocodylidae (*Crocodylus porosus* [saltwater crocodile; 74×]), and Gavialidae (*Gavialis gangeticus* [Indian gharial; 81×])(Wan et al. 2013; Green et al. 2014; Putnam et al. 2016) and cryptodiran turtles from the clades Testudinoidea (*Chrysemys picta* [Emydidae; painted turtle; 15×, improved with cytogenetic mapping]), Americhelydia (*Chelonia mydas* [Cheloniidae; green sea turtle; 110×]) and Trionychia (Trionychidae; *Pelodiscus sinensis* [Chinese softshell turtle; 105×], *Apalone spinifera* [spiny softshell turtle; 33.4×])(Wang et al. 2013; Badenhorst et al. 2015), along with outgroup taxa for comparison. I used a combination of gene predictions and BLAST searches against genomic contigs to determine the presence and functionality of 20 genes related to light-sensitivity (supplementary table S1 and dataset S1, Supplementary Material online).

Turtle Visual Opsins

Vertebrate phototransduction takes place in the rod and cone cells of the retina. Both cell types possess photosensitive pigments comprised of proteins called opsins covalently bound to retinoid chromophores. Upon absorbing light, these pigments initiate a phototransduction cascade that culminates in electrical signaling to the brain, resulting in vision. The ancestral vertebrate likely had five visual opsins, one expressed in the dim-light adapted rods (RH1), and four expressed in separate bright-light (photopic) adapted cone cells (SWS1, SWS2, RH2, and LWS), the latter allowing for photopic color discrimination (Davies et al. 2012).

Chrysemys picta and *Chelonia mydas*, possess all five visual opsins, suggesting that tetrachromatic color vision was the ancestral state for Durocryptodira and, by extension, Testudinata. All four turtle species retain genes encoding RH1 (rod opsin) as well as two classes of cone opsin (RH2 [rod-like cone opsin], LWS [long wavelength-sensitive opsin]). Both trionychid species show evidence of loss or inactivation of *SWS1* (encodes short wavelength-sensitive opsin 1). *Pelodiscus sinensis* has a 19-bp deletion at the intron 1–exon 2 boundary and *Apalone spinifera* returned negative BLAST results. The relatively low coverage (33.4×) assembly for *A. spinifera* includes many small contigs, raising the possibility that its absence may be due to an assembly error. However, the genes that flank *SWS1* in zebra finch, human and anole (*FLNC*, *CALU*) were recovered, suggesting whole gene deletion is probable. While *A. spinifera* retains *SWS2* (encodes short wavelength-sensitive opsin 2), in *P. sinensis* it is highly unusual and suggestive of pseudogenization or neofunctionalization. Exon 4 has an 18-bp deletion and an apparent premature stop codon, though the alignment is ambiguous and there is a potential alternative splice donor site that eliminates the stop codon. Additionally, in place of the canonical stop codon, there is a 1,293-bp extension of the gene, more than doubling the length of the coding sequence. This region has a repetitive motif, and upon BLASTing it against GenBank, its highest similarity (*E* value 8e−43; Query cover: 97%; Ident: 67%) is to a predicted cardiomyopathy-associated protein 5-like gene in *Acinonyx jubatus* (cheetah; XM_015088347). dN/dS ratio branch test analyses of *SWS2* provide evidence of an elevated rate of protein evolution (foreground $\omega = 0.2044$; background $\omega = 0.0473$; $P < 0.05$; supplementary table S2, Supplementary Material online). A branch-sites test failed to find evidence of positive selection, suggesting that the elevated rate is due to relaxed selection, consistent with pseudogenization. While this anomaly may be due to an assembly error, further research should explore if SWS2 in *Pelodiscus* has a modified function or is lost entirely.

Earlier microspectrophotometry (MSP) studies found only three cone pigments in the durocryptodirans *Trachemys scripta* (pond slider; Emydidae), *Chelonia mydas* and *Mauremys reevesi* (Chinese pond turtle; Geoemydidae) (Liebman and Granda 1971; Ohtsuka 1985), likely corresponding to SWS2 (λ_{max} [peak absorbance wavelength] 440–460 nm), RH2 (λ_{max} 502–540 nm), and LWS pigments (λ_{max} 562–620 nm) based on the typical λ_{max} values of these pigments (Davies et al. 2012). However, Loew and Govardovskii (2001) found an additional ultraviolet photoreceptor in *T. scripta*, probably representing an SWS1 pigment (λ_{max} 372 nm; Davies et al. 2012). This was not observed by Liebman and Granda (1971), likely due to a failure to examine the ultraviolet part of the spectrum (Loew and Govardovskii 2001). SWS1 pigments in both *Chrysemys picta* and *Chelonia mydas* are predicted to be ultraviolet-sensitive based on the presence of F86, S90, and M93 and T93, respectively [supplementary table S3, Supplementary Material online; reviewed in Emerling et al. (2015)]. Though both MSP (Liebman and Granda 1971) and electroretinography (ERG; Levenson et al. 2004) studies failed to find definitive evidence of UV-sensitive cones in *C. mydas*, ERG measurements suggest an increase in sensitivity towards the UV, and a behavioral study on hatchling *C. mydas* indicates that they are capable of perceiving UV light (Witherington and Bjorndal 1991). dN/dS ratio analyses and ancestral sequence reconstructions (supplementary tables S2 and S4, Supplementary Material

Table 1. Summary of Shared Inactivating Mutations in Focal Taxa

RH2	Exon 1	Exon 2–Intron 3		
Crocodylia	Deleted	55-bp deletion		
OPN4M	Exon 1	Intron 6	Exon 7	Exon 8
Crocodylia	Start codon mutation	Splice donor mutation	1-bp deletion	Two premature stop codons
EEVS-like	Exon 2	Exon 3	Intron 3	
Crocodylia	*Chompy* repeat element insertion, three 1-bp deletions, 1-bp insertion, two premature stop codons	Two 1-bp deletions	Splice donor mutation	
MT-Ox	Exon 1	Exon 2	Exon 4	Exon 7
Crocodylia	1-bp insertion, 8-bp deletion	1-bp deletion	Two 8-bp deletions, 1-bp deletion	1-bp deletion
OPNP	Exon 2	Exon 4		
Alligator	7-bp deletion	4-bp deletion		
OPNPP	Exon 1	Exon 2		
Crocodylia	Three 1-bp deletions	No BLAST results		
Cyptodira	Two 1-bp deletions	Two premature stop codons		
OPNPT	Exon 1	Exon 2	Exon 3	
Crocodylia	No BLAST results	1-bp insertion, three premature stop codons	No BLAST results	
Aves	Start codon mutation, three 1-bp deletions, 23-bp deletion	No BLAST results	No BLAST results	
Cryptodira			1-bp deletion	

online) provide some evidence of visual adaptation in testudine history. Branch-sites tests estimated positive selection on *LWS* on the stem Cryptodira branch, and substitutions known to influence visual pigment spectral sensitivity (Yokoyama 2008) occurred on several branches: SWS1, Durocryptodira (T52V), *Chrysemys* (T93M, A97S, and V109A); SWS2, Durocryptodira (S91T), *Chelonia* (A116T and S292A); RH2, *Chelonia* (A164S). Between the putative loss of short-wavelength sensitive pigments in the two trionychian species and key tuning site substitutions in these pigments in durocryptodirans, it seems probable that there have been strong selective pressures on these pigments during testudine history. This may be due in part to the higher abundance of light with longer wavelengths in freshwater habitats. The low number of putative adaptive changes in the visual opsin system in stem turtles may be partially due to a reliance on switches in opsin chromophores rather than on substitutions in opsin amino acids to tune color vision. The retinoid chromophore comes in two forms: a vitamin A_1-derived chromophore leads to a more blue-shifted pigment, whereas a vitamin A_2-derived chromophore produces a red-shifted pigment (Enright et al. 2015). Liebman and Granda (1971) found that the saltwater *Chelonia mydas* possessed the former, and the freshwater *Trachemys scripta* possessed the latter. This distinction is also found in saltwater vs. freshwater fishes and is thought to be an adaptation to the respective blue- and red-shifted waters they inhabit (Beatty 1984). Perhaps as stem turtles adapted to freshwater, they experienced minimal adaptations to their visual opsin genes because they switched to a vitamin A_2-derived chromophore. Sea turtles subsequently reverted to a vitamin A_1 chromophore, and the three spectral tuning site substitutions estimated in *C. mydas*' cone opsins might be adaptations for vision in marine habitats.

Crocodylian Visual Opsins

In all four sampled crocodylian species, I recovered two intact cone opsin genes (*SWS2* and *LWS*) and the rod opsin gene *RH1*, suggestive of dichromatic photopic color vision. *Alligator sinensis* has a deletion at the intron 3–exon 4 boundary of *RH1*, suggesting that it has become inactivated. A branch test of *RH1* did not find a significantly higher dN/dS ratio in *A. sinensis* compared with the background (supplementary table S2, Supplementary Material online), and gene prediction suggests that the rod phototransduction genes are intact, indicating that if this mutation is real, it is very recent or has not led to the loss of RH1 function. Given that the loss of *RH1* is exceptionally rare, with strong evidence of absence only in cave fishes (Niemiller et al. 2013), a gecko (Liu et al. 2015) and a snake (Simões, Sampaio, Loew, et al. 2016), this should be tested with more data. Synteny information provides evidence that *SWS1* is deleted in crocodylians. As described above, *FLNC* and *CALU* flank *SWS1* in amniotes, and both genes were found in all four crocodylians. However, they were never recovered on the same contig, making it difficult to completely rule out assembly errors. I recovered a highly fragmentary *RH2* in the genomes of all four crocodylians. Beyond sequence homology, identity of *RH2* is confirmed by gene tree estimation (supplementary fig. S1, Supplementary Material online) and synteny: it is flanked by *MLN* and *GRM4* in *Gallus gallus* (chicken) and *Pelodiscus sinensis*, and both of these genes flank *RH2* on an *Alligator mississippiensis* contig. All four crocodylian *RH2* sequences share inactivating mutations (table 1), suggesting pseudogenization in a common ancestor.

Despite the inference that only two cone opsin genes were retained in the ancestral crocodylian, previous MSP experiments in crocodylians suggest that the number of cone types

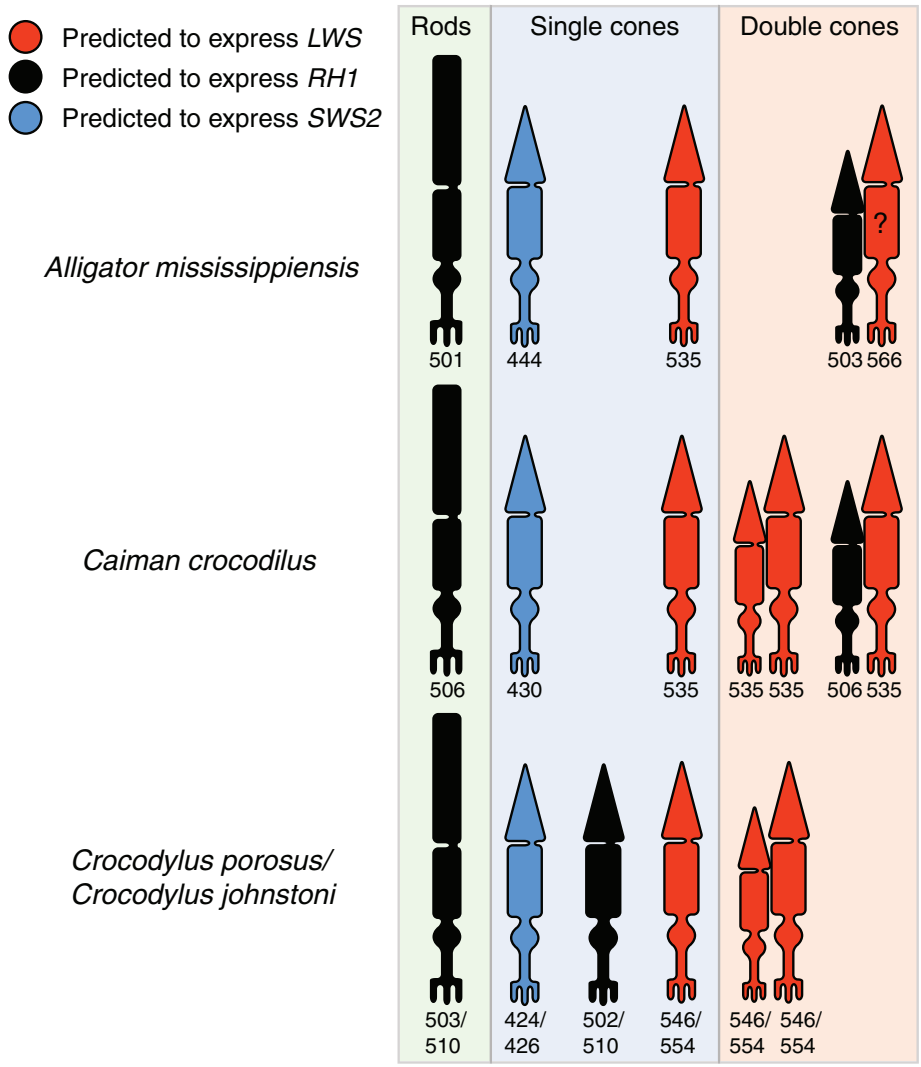

FIG. 1. Diagrams of crocodylian retinal photoreceptors [based on Govardovskii et al. (1988), Sillman et al. (1991), and Nagloo et al. (2016)] and their predicted constituent opsin pigments. Numbers below photoreceptors indicate λ_{max} (peak absorption wavelength).

ranges from three to four (fig. 1). *Caiman crocodilus* (spectacled caiman), *Alligator mississippiensis*, *Crocodylus porosus*, and *Crocodylus johnstoni* (freshwater crocodile), all have single cones with pigments measured at λ_{max} of 424–444 nm (Govardovskii et al. 1988; Sillman et al. 1991; Nagloo et al. 2016). Only SWS1 and SWS2 pigments are known to peak in this range (Davies et al. 2012), and given the absence of *SWS1* in crocodylian genomes, this implies that these single cones express the SWS2 opsin. A second single cone type has a λ_{max} of 535–554 nm, a spectral tuning position typically occupied by LWS pigments in vertebrates (Davies et al. 2012). Using Yokoyama (2008), five-sites rule to predict LWS λ_{max} (supplementary table S3, Supplementary Material online) and assuming a vitamin A_1-derived chromophore, *A. mississippiensis* is expected to have a λ_{max} of 532 nm, very close to the 535 nm peak measured by MSP (Sillman et al. 1991). The *C. porosus* LWS pigment is predicted to have a λ_{max} of 545 nm, nearly identical to the 546 nm pigment in cones measured by Nagloo et al. (2016). Both *Crocodylus* species and *Caiman crocodilus* also have double cones with both members expressing pigments with a λ_{max} identical to the LWS single cones (Govardovskii et al. 1988; Nagloo et al. 2016). *A. mississippiensis*, however, has a pigment with a λ_{max} of 566 nm in the principal member of its double cone, which is red-shifted relative to its presumptive LWS single cones (Sillman et al. 1991). I did not discover a second LWS opsin gene in the genome of this species, suggesting that this spectral shift may be accomplished by changing the ratio of vitamin A_1 to A_2. Nagloo et al. (2016) used modeling to predict that *C. johnstoni* has a mixture of A_1-/A_2-derived chromophores, rendering its LWS cones red-shifted relative to those of *C. porosus*. However, Sillman et al. (1991) reported that none of the photoreceptor pigments they measured in *A. mississippiensis* fit an A_2 curve, bringing this hypothesis into question. Nonetheless, because *A. mississippiensis* is a freshwater species, it suggests that this is a viable possibility.

A third cone pigment has been discovered in crocodylians that remains unaccounted for. This pigment's λ_{max} ranges from 502 to 510 nm and has been found in a third class of single cone in *Crocodylus porosus* and *C. johnstoni* (Nagloo et al. 2016), the double cone accessory member in *Alligator mississippiensis* (Sillman et al. 1991), and one of two types of

double cone accessory members in *Caiman crocodilus* (Govardovskii et al. 1988). This peak absorbance is typically associated with RH2 pigments (Davies et al. 2012), yet *RH2* is pseudogenized in crocodylians. I hypothesize that these are rod opsin (RH1) pigments, which have been co-opted into these cones. As noted above, *RH1* is present in all four crocodylian species I examined, with the possible exception of *Alligator sinensis*, and MSP measurements of the rod pigments reveal λ_{max} values consistent with RH1 (Davies et al. 2012). Importantly, the rod and putative RH1 cone pigments have nearly, or exactly, identical λ_{max} measurements in all four species (fig. 1): *Alligator mississippiensis* rod $\lambda_{max} = 501$ nm, putative RH1 cone $\lambda_{max} = 503$ nm; *Caiman crocodilus* rod $\lambda_{max} = 506$ nm, putative RH1 cone $\lambda_{max} = 506$ nm; *Crocodylus porosus* rod $\lambda_{max} = 503$ nm, putative RH1 cone $\lambda_{max} = 502$ nm; *Crocodylus johnstoni* rod $\lambda_{max} = 510$ nm, putative RH1 cone $\lambda_{max} = 510$ nm (Govardovskii et al. 1988; Sillman et al. 1991; Nagloo et al. 2016).

While some vertebrates, particularly colubroid snakes (Schott et al. 2015; Simões, Sampaio, Douglas, et al. 2016), possess rod-like (transmuted) cones expressing cone opsins and cone-like rods expressing rod opsin, the condition in crocodylians appears unprecedented in two ways. The first is the presumed expression of *RH1* in a class of true cones. Alternatively, the putative RH1 single cones may simply be cone-like rods, but this posits that some rods became cone-like while others retain their original morphology. Walls (1942, p. 615) stated that the *Alligator mississippiensis* retina includes some very rod-like cones near the tapetal region of the retina, giving some credence to the latter hypothesis. Ultrastructural examinations of these putatively RH1 cones and immunohistochemical staining of cone phototransduction elements are instrumental in testing these hypotheses. The second apparently unique trait is the putative expression of *RH1* in double cones alongside a cone opsin (*LWS*). This could also be verified with immunohistochemistry to rule out the possibility that this is another opsin. Both of these traits are extremely unusual and warrant further investigation. This hypothesis has an analog in lissamphibians: frogs and salamanders possess two spectral classes of rods, known as red and green rods. Red rods express the typical RH1, whereas green rods have co-opted the cone opsin SWS2 (Ma et al. 2001). If this hypothesis withstands further scrutiny, crocodylians would provide a counterpart to the state in lissamphibians, and continue to demonstrate the remarkable evolutionary lability of vertebrate photoreceptors.

Because single cones contribute to color vision but double cones are thought to only provide achromatic information (Bowmaker 2008; though see Pignatelli et al. 2010), expressing *RH1* in the accessory members of alligator and caiman cones likely does not affect color discrimination. However, the presence of RH1-expressing single cones in both *Crocodylus johnstoni* and *Crocodylus porosus*, would imply that crocodylids, at least since the common ancestor of *Crocodylus* (Oaks 2011), have recovered trichromatic color vision. In mammals, several lineages of primates have regained trichromatic color vision either via allelic variants of *LWS* (platyrrhines, lemuriforms) or the duplication of *LWS* (*Alouatta*, catarrhines; Davies et al. 2012). Some species of snakes are predicted to have regained trichromatic color vision by modifying their rod photoreceptors to be more cone-like (Schott et al. 2015; Simões, Sampaio, Douglas, et al. 2016). The condition in *Crocodylus* would seem to represent a novel pathway of reinventing trichromatic color vision in amniotes.

Branch-sites tests estimated that *LWS* underwent positive selection on the stem crocodylian branch, and ancestral sequence reconstructions point to several tuning site changes (supplementary tables S2 and S4, Supplementary Material online): SWS2, Crocodylia (A116T, S292A); LWS, Crocodylia (S180A, Y277F), *Alligator* (T285A). The SWS2 substitutions are identical to those of *Chelonia mydas*, possibly indicating adaptive convergence. On the stem Crocodylia branch, LWS is predicted to have shifted from a λ_{max} of 560 nm to a λ_{max} of 545 nm with a further blue-shifting on the stem *Alligator* branch to 532 nm. RH1 also experienced substitutions at site 13 on the stem Crocodylia (M13L) and *Alligator* (L13F) branches. This site is not known to affect spectral tuning, but it does appear to affect glycosylation of RH1 (Fernández-Sampedro et al. 2016). Notably, site 13 is conserved as methionine in all of the outgroup taxa in this study (supplementary table S3, Supplementary Material online), whereas therian mammals independently experienced a M13F substitution that was estimated to have been under positive selection (Fernández-Sampedro et al. 2016).

Light-Associated Gene Loss and the Crocodylian Nocturnal Bottleneck

In addition to the loss of two cone opsins, I found evidence that seven additional light-associated genes have become inactivated or deleted in crocodylians. *OPN4M*, *EEVS*-like, and *MT-Ox* each have numerous inactivating mutations shared among all four crocodylian species (table 1), providing strong evidence of pseudogenization in their common ancestor. *OPNP* is a pseudogene in all four species, but only the two *Alligator* species share inactivating mutations (table 1), possibly suggesting independent loss in Alligatorinae, Gavialidae and Crocodylidae. However, through a series of nested dN/dS ratio models, I found that each of the crown branches had dN/dS ratios that were not significantly different from a neutrally evolving value of 1, the sole exception being the stem Crocodylidae + Gavialidae branch using the F1X4 codon frequency model. When the crown Crocodylia branches were grouped together as one ratio, ω was estimated to be 1.2062–1.3503 (not significantly different from 1; $P > 0.25$), consistent with a hypothesis of relaxed selection in crown Crocodylia. Using F1X4, the stem crocodylian ω (0.2382) was nearly significantly higher than the background (0.1212; $P = 0.051$), whereas a second model (CodonFreq = 2) found the difference to be significant (0.2373 vs. 0.0959; $P = 0.014$; supplementary table S5, Supplementary Material online), lending more credence to the hypothesis of *OPNP* loss in a common ancestor. *OPN5L2* was not recovered via NCBI's predictive pipeline or by directly BLASTing against NCBI's whole genome shotgun assembly contigs database (WGS). *OPN5L2* in the zebra finch and *Pelodiscus sinensis* is flanked by *CDC5L* and

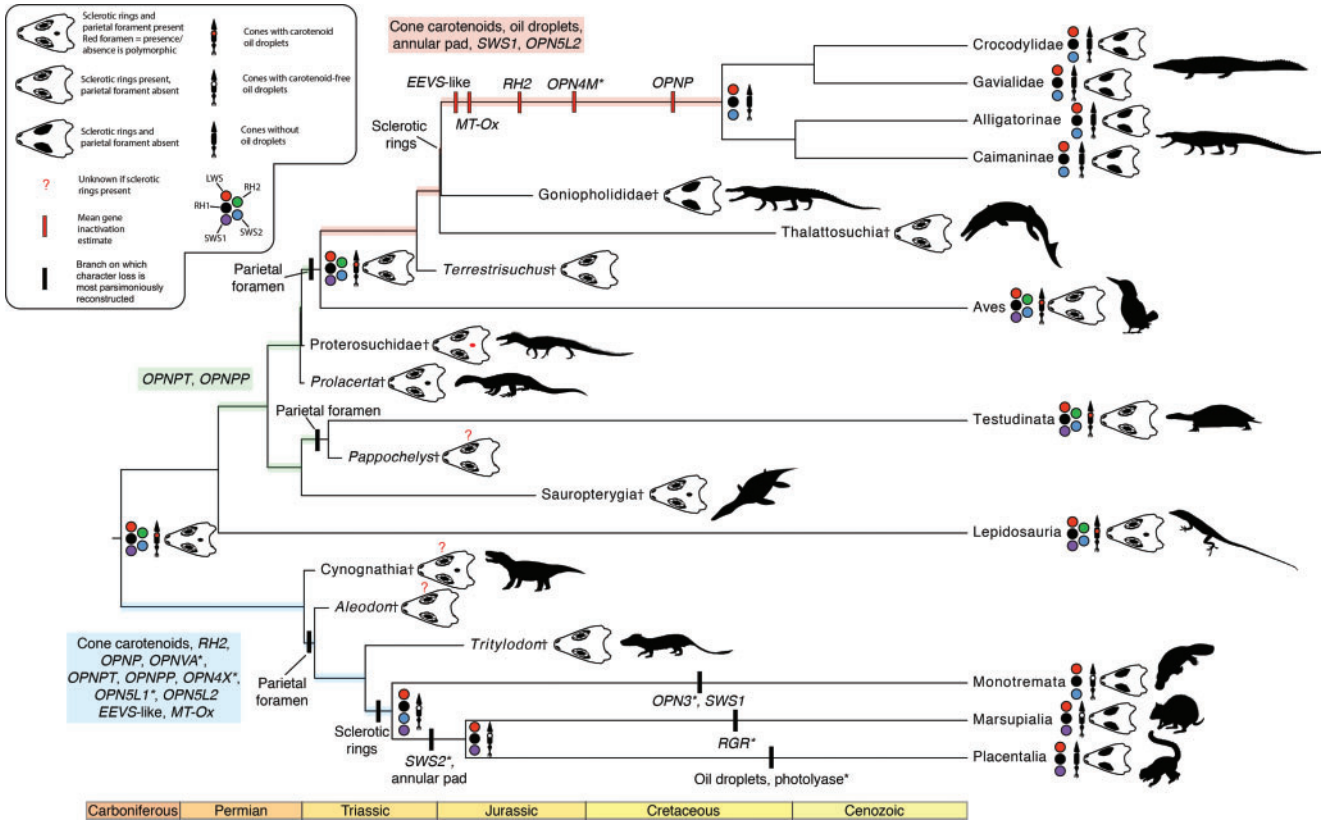

Fig. 2. Timetree demonstrating the loss of various traits associated with photoreception in amniotes. Character states at terminal nodes represent most parsimonious ancestral state for that taxon, not necessarily the state for all members of the clade. Fossil taxa branch lengths are based on occurrences in the paleobiology database (i.e., they begin at the first appearance of the taxon in the fossil record), and therefore their times of divergence from crown lineages are probably underestimated. Highlighted branches indicate uncertainty of the timing of trait loss on the stem mammalian (blue) and crocodylian branches (red), and the loss of *OPNPP* and *OPNPT* in archelosaurs (green). Both genes are depicted as being lost at minimum concurrently with the parietal foramen (see text). Asterisks indicate characters that are lost uniquely on the phylogeny. Silhouettes from phylopic.org (supplementary table S7, Supplementary Material online).

MUT, and both genes were recovered from the same contig in *Alligator mississippiensis*, suggesting *OPN5L2* was deleted in crocodylians. *OPNPT* and *OPNPP* were inactivated in crocodylians, birds and turtles and will be discussed separately below.

All of the genes described above or, in one case, closely related paralogs (*OPN4X*) were also independently lost on the stem mammalian lineage, and all of them have a function known or predicted to be associated with light exposure. Pinopsin (*OPNP*) is a light-sensitive pigment expressed in the pineal of lizards (Frigato et al. 2006; Su et al. 2006; Wada et al. 2012) and birds (Okano et al. 1997), likely being important for melatonin secretion (Frigato et al. 2006). Notably, crocodylians are reported to completely lack a pineal (Roth et al. 1980), correlating, potentially causally, with the inactivation of *OPNP* in this clade. Mammals also lack *OPNP* (Gerkema et al. 2013), despite retaining a pineal gland. However, during mammalian evolution, the pineal migrated from a superficial portion of the brain to a deeper region that is less penetrable to light (Falcón et al. 2009), thereby losing its direct photosensitivity.

There are two vertebrate melanopsins, both of which are photosensitive: OPN4M (mammal-like melanopsin) and OPN4X (*Xenopus*-like melanopsin). Both are expressed in a variety of tissues in nonmammalian vertebrates, including the eye, brain, pineal, and skin (Bellingham et al. 2006), with OPN4M known to entrain circadian rhythms and modulate the pupil response in mammals (Hankins et al. 2008). Though *OPN4X* is absent from mammalian genomes (Bellingham et al. 2006), *OPN4M* was inactivated in crocodylians. It is unclear whether lineage-specific selection pressures led to the loss of *OPN4M* and *OPN4X* in crocodylians and mammals, respectively, or if these genes are in some ways functionally redundant, allowing for the loss of either gene.

OPN5L2 (neuropsin-like 2) is a photosensitive opsin expressed in the chicken retina, brain and especially the adrenal glands (Tomonari et al. 2008; Ohuchi et al. 2012). Adrenal expression suggests that this gene may be involved in seasonal changes in sex hormone production. Mammals lack the gene encoding this opsin and a paralog, *OPN5L1*. *EEVS*-like and *MT-Ox* were recently discovered to encode enzymes responsible for synthesizing gadusol, a compound that protects against ultraviolet radiation (Osborn et al. 2015). As in crocodylians, both genes are absent in mammals.

In addition to these genes, crocodylians lost several anatomical features associated with high acuity color vision in sauropsids, including sclerotic rings, an annular pad of the lens and colored cone oil droplets (fig. 2). Sclerotic rings are thought to stabilize the eye against changes in intraocular

pressure during accommodation (Walls 1942), and because high acuity vision, including accommodation, is largely associated with bright light conditions, the loss of sclerotic rings is typically thought to correlate with adaptation to dim light (Walls 1942; Atkins and Franz-Odendaal 2016). Nesbitt et al. (2013) showed that while various early crocodylomorphs, including *Terrestrisuchus*, Thallatosuchia, and Pholidosauridae, had sclerotic rings, more crownward lineages, such as Goniopholididae and *Shamosuchus*, appear to have lacked them. The absence of sclerotic rings in fossils does not definitively confirm their absence, because the delicate component ossicles are not always preserved. Nonetheless, the convincing absence of these rings in Goniopholididae, a taxon that appears in the fossil record 199.3 Ma (Paleobiology Database; PBDB; https://paleobiodb.org [last accessed June 2016]), provides a minimum age by which this trait was lost. Pholidosauridae first appears 174.1 Ma and Thalattosuchia is recorded as early as 199.3 Ma (PBDB), preventing any additional temporal resolution to the loss of this trait. I was able to date the inactivation of five genes (supplementary tables S5 and S6, Supplementary Material online), and all point estimates postdate the origin of Goniopholididae (fig. 2): 193.9 Ma (*EEVS*-like), 189.2 Ma (*MT-Ox*), 169.6 Ma (*RH2*), 148.7 Ma (*OPN4M*), and 111.8 Ma (*OPNP*; assumes inactivation in the stem crocodylian). Notably, the genes encoding the gadusol synthesis pathway, *EEVS*-like and *MT-Ox*, had extremely similar estimates for inactivation, a prediction that follows their shared function. Together, these data suggest a long period of dim-light adaptation in crocodylians that dates at least to the early Jurassic, coeval with the mammalian nocturnal bottleneck (fig. 2).

Gene Inactivation and the Loss of the Parietal ("Third") Eye in Turtles and Archosaurs

OPNPP (parapinopsin) and *OPNPT* (parietopsin) are not only inactivated in crocodylians, but also testudines and birds. Both genes have shared inactivating mutations in all four crocodylian species and all four testudines (table 1), respectively, providing a minimum point of inactivation in a stem crocodylian and stem cryptodire. In all of the birds examined, *OPNPT* is a pseudogene with shared inactivating mutations (table 1), and although the coding sequence for *OPNPP* was not recovered, a conserved region 5′ of the start codon was found in all of the taxa I examined. In the anole, *OPNPP* is flanked by *CACNA2D3* and *ACTR8*, both of which appear to be flanking this fragment in *Aquila chrysaetos* (golden eagle; supplementary table S1, Supplementary Material online). For both genes, the avian taxon sampling included a palaeognath (*Apteryx australis*; Southern brown kiwi) and several neognaths, suggesting that both were deleted/inactivated in a stem avian. For *OPNPP*, exons 1–3 were recovered in at least two turtles, but only exon 1 was obtained for crocodylians. None of the overlapping sequences possess unambiguous shared inactivating mutations, precluding the ability to confirm inactivation in the archelosaurian common ancestor. *OPNPT* similarly had minimal overlap between archelosaurian taxa, and not even birds and crocodylians had overlapping sequences, making it unclear if there are any shared archosaurian inactivating mutations. While nested dN/dS ratio models provide evidence of relaxed selection in crown Archelosauria (supplementary table S5, Supplementary Material online; *OPNPP* ω: 0.8084-0.9306; *OPNPT* ω: 0.7424–0.9244; both not significantly different from 1), the stem Archelosauria branch in each case had an ω estimated at 999 (N*dN = 30.6-44.3; N*dS = 0.0), suggesting that this branch experienced positive selection prior to being lost, as opposed to a transition from purifying to relaxed selection. Based on the available data and analyses, it can confidently be assumed that both genes were lost at minimum on the stem crocodylian, avian and testudine branches and at most on the stem archelosaurian branch (fig. 2). Both genes were also lost in parallel in mammals (Gerkema et al 2013), suggesting that similar selective pressures may have acted in these lineages.

Parapinopsin was discovered originally in the catfish parapineal and pineal organs, and later found in the lamprey, trout, and frog pineal (Kawano-Yamashita et al. 2014). Among amniotes, it is expressed in the green iguana (*Iguana iguana*) parietal eye (Wada et al. 2012), consistent with evidence that the parapineal organ and parietal eye are homologous (Kappers 1965). Parietopsin was discovered in the side-blotched lizard (*Uta stansburiana*) parietal eye (Su et al. 2006), and was later confirmed to be present in the same organ in iguanas (Wada et al. 2012). Given the expression patterns of these genes in squamates, their loss in both archelosaurians and mammals (Gerkema et al. 2013) may be linked to the elimination of the parietal eye in these clades.

Squamates that possess a parietal eye also possess a parietal (pineal) foramen in their skulls, allowing for connection between the parietal eye and the pineal gland. Although this osteological feature is absent from modern archelosaurians and mammals, many stem taxa possessed this foramen and presumably a parietal eye with it. Numerous stem mammal lineages, including caseids, gorgonopsians, and cynognathians possessed a parietal foramen, whereas Triassic probainognathians, including mammals, lack(ed) this trait (Schoch and Sues 2015; Benoit et al 2016). The absence of a parietal foramen is generally considered a synapomorphy for Archosauriformes [Nesbitt et al. 2015; though see Ezcurra and Butler (2015) for evidence of parietal foramen polymorphism in proterosuchids], a clade that includes archosaurs (Nesbitt 2011), whereas the more inclusive clade Archosauromorpha includes extinct taxa that retained the parietal foramen (rhynchosaurs, trilophosaurids, and azendohsaurids). The stem testudine *Proganochelys* (~220 Ma) and the earlier *Pappochelys* (~240 Ma) both lack a parietal foramen (Schoch and Sues 2015), whereas the putative stem turtle *Eunotosaurus* (~260 Ma) retains this structure. The association of the latter species with turtles, however, is contentious because it is frequently recovered in phylogenetic analyses with parareptilians (Lee 2013). Alternatively, recent analyses have frequently recovered sauropterygians (e.g., placodonts, plesiosaurs) as the sister group to crown and stem testudines (Lee 2013), and sauropterygians often retained a parietal foramen. Together, these provide evidence that the parietal eye, along with *OPNPP* and *OPNPT*, was lost in parallel in stem archosaurs and testudines.

The parietal eye is a photoreceptive organ (Eakin 1973) that appears to be closely linked to regulation of body temperature in ectothermic squamates (Stebbins and Eakin 1958; Hutchison and Kosh 1974; Phillips and Harlow 1981), likely through regulating melatonin secretion (Firth and Kennaway 1980). It is frequently absent in nocturnal and fossorial species, as well as those at lower latitudes (Gundy and Ralph 1975), suggesting that thermal stability might be an important factor selecting for its loss. If true, its parallel loss in archosaurs and mammals may be tied to the evolution of elevated metabolic rates in these lineages (Benoit et al. 2016; Legendre et al. 2016). In turtles, a hypothesized fossorial origin for this lineage (Lyson et al. 2016) may explain the loss of the parietal eye, because spending an increasing amount of time underground may render its function obsolete. Alternatively, it may have not been fossoriality *per se* that led to the loss of the parietal, but the proposed mode of digging (Lyson et al. 2016), which involves fixing the skull to the roof of the burrow to stabilize the body. Presumably this would lead to repeated damage of the parietal eye, selecting for regression of this character.

Conclusions

The origins of the archelosaurian clades Testudinata and Crocodylia likely included transitions into niches that influenced their respective visual systems. Turtles probably underwent adaptations to freshwater habitats, and crocodylians show anatomical modifications suggestive of a long period of nocturnal adaptation. Consistent with these hypotheses, here I reported evidence of modifications and losses of the short-wavelength sensitive visual opsins in turtles and the loss of visual opsins, nonvisual opsins, and sunscreen enzymes in crocodylians. A combination of genomic and microspectrophotometry data suggests that crocodylians have co-opted the rod opsin (RH1) for single and double cone functions, implying reacquisition of trichromacy in crocodiles via a novel mechanism. Finally, the losses of parietopsin and parapinopsin in crocodylians, turtles, and birds correlate with the loss of the parietal eye in the fossil records of these clades. Together, these data provide greater evidence of the lability of the visual system in vertebrates and further demonstrate the power of comparative genomics to corroborate the fossil record in providing a record of adaptive events early in amniote history.

Materials and Methods

I searched the genomes of crocodylians and turtles (accession numbers in supplementary table S1, Supplementary Material online) using two approaches. The first utilized NCBI's Eukaryotic Genome Annotation (EGA) pipeline. EGA is currently available for two crocodylians (*Alligator mississippiensis*, *Alligator sinensis*) and three testudines (*Chelonia mydas*, *Chrysemys picta*, and *Pelodiscus sinensis*). These taxa, along with two avian outgroup species (*Gallus gallus*, *Taeniopygia guttata*), were examined for the presence and functionality of 20 genes. EGA provides evidence of nonfunctionality/absence of genes in two ways: negative BLAST results (i.e., no gene prediction was possible) or by providing an annotation indicating the gene encodes a "Low quality protein". If neither of these outcomes occurred, the gene of interest was assumed to encode a functional transcript.

In cases where EGA provided evidence of nonfunctionality, I designed *in silico* probes to obtain sequences directly from NCBI's whole genome shotgun contig (WGS) database. To design the probes, I first obtained reference mRNA sequences from GenBank, with the exception of *EEVS*-like. No mRNA sequences are available for *EEVS*-like so I used a predicted sequence following Osborn et al. (2015). I then BLASTed (megablast) the reference sequences against a reference genome (WGS) to obtain a contiguous sequence encompassing exons, introns and 5′ and 3′ flanking DNA. The contiguous sequence was aligned to the reference sequence using Muscle (Edgar 2004) in Geneious version 9.1.2 (Kearse et al. 2012), manually adjusted to allow for exon annotation, and was subsequently used as a probe to capture sequences of the taxa of interest by BLASTing (discontiguous megablast) against WGS. In cases of negative BLAST results, I relaxed the search parameters and/or used alternative probes from more closely related taxa. For examples in which I was unable to obtain sequences from any crocodylian species, I used synteny data from amniote taxa in Ensembl to test for evidence of gene deletion. The resulting BLAST hits were aligned to the reference sequence and examined for inactivating mutations (e.g., premature stop codons, frameshift indels, splice site mutations, and start codon mutations).

I searched for relevant genes in the genomes of four crocodylians (*Crocodylus porosus*, *Gavialis gangeticus*, *Alligator mississippiensis*, and *Alligator sinensis*) and four testudines (*Chrysemys picta*, *Chelonia mydas*, *Pelodiscus sinensis*, and *Apalone spinifera*). For *OPNPT* and *OPNPP*, several avian genomes were additionally queried. The genes of interest include *SWS1*, *SWS2*, *RH1*, *RH2*, *LWS*, *OPNP*, *OPNPT*, *OPNPP*, *OPNVA* (vertebrate ancient opsin), *OPN4X*, *OPN4M*, *OPN3* (encephalopsin), *OPN5* (neuropsin), *OPN5L1* (neuropsin-like 1), *OPN5L2*, *RRH* (peropsin), *RGR* (retinal G protein-coupled receptor), *EEVS*-like, *MT-Ox*, and the gene encoding photolyase. Visual opsin tuning sites were obtained from Yokoyama (2008).

In instances where one or more species showed evidence of pseudogenization, I performed gene inactivation dating estimates as detailed in Meredith et al. (2009) with some modifications. In addition to removing codon positions with ambiguous homology, I deleted every codon position that was not present in at least one of the pseudogenic sequences. Because dN/dS ratios can differ across a gene, this ensured comparisons solely between the sites for which I had data for the focal taxa. For *MT-Ox*, I deleted exon 6 in the analyses because it is an ultra-conserved element and therefore unlikely to evolve under relaxed selection. I compared models with estimates of branches putatively under relaxed selection to models under which the branch ω was fixed at 1. If they were not significantly different, I used the mixed branch ω estimates from the latter models (ω fixed at 1) for gene inactivation calculations. The ages of crown Crocodylia and Archosauria were assumed to be 92.84 Ma (Oaks 2011; four analyses mean) and 245 Ma (Shedlock and

Edwards 2009; timetree.org [last accessed June 2016], median age), respectively. dN/dS ratio analyses for dating gene inactivations, branch tests, branch-sites tests and ancestral sequence reconstructions were performed with PAML ver. 4.8 (Yang 2007). Branch and branch-site tests allow for dN/dS ratio models whereby ω is estimated on assigned branches in a phylogeny. Branch tests assume a single ω for the entire gene, whereas branch-site tests allow for the gene to be broken up into purifying, relaxed and positive selection categories. Branch-sites tests and ancestral sequence reconstructions implemented the F3X4 (CodonFreq = 2) codon frequency model. Gene inactivation estimate analyses implemented both F1X4 (CodonFreq = 1) and F3X4 codon frequency models. F1X4 calculates codon frequencies from average base compositions, and F3X4 does so using average base compositions at the different codon positions. The topologies used in the analyses are based on Chiari et al. (2012), Oaks (2011), and Crawford et al. (2015).

I estimated a phylogeny of the five visual opsins, *OPNP*, *OPNPP*, *OPNPT*, *OPN4M*, and *OPN4X* to verify the orthology of the Archelosaurian visual opsins and opsin pseudogenes (supplementary fig. S1, Supplementary Material online). Alignments of each opsin were aligned successively using the Translation alignment tool in Geneious and adjusted manually. A phylogeny was estimated using RAxML (Stamatakis 2014) with the GTRGAMMA model on CIPRES (phylo.org; last accessed September 2016; HPC2 on XSEDE), and included 500 bootstrap replications using the GTRCAT model.

I predicted the λ_{max} of SWS1 and LWS pigments in testudines and crocodylians, respectively, using key tuning sites known to confer spectral sensitivity (Yokoyama 2008). Though it is not currently feasible to perfectly predict λ_{max}, assigning ultraviolet vs. violet sensitivity in vertebrates is generally reliable (Yokoyama 2008; Hauser et al. 2014; see Emerling et al. 2015, supplementary tables S1 and S5, Supplementary Material online), and the "five-sites rule" for LWS allows for greater precision in estimating λ_{max} for this opsin (Yokoyama 2008).

Supplementary Material

Supplementary data are available at *Molecular Biology and Evolution* online.

Acknowledgments

I thank David Gower, an anonymous reviewer, and the MBE editorial team for helpful comments on the manuscript and Michael Nachman for helpful discussions. This research was supported by an National Science Foundation (Div of Biological Infrastructure) Postdoctoral Research Fellowship in Biology (Award #1523943).

References

Anquetin J. 2011. Evolution and palaeoecology of early turtles: a review based on recent discoveries in the Middle Jurassic. *Bull La Soc Geol Fr.* 182:231–240.

Atkins JB, Franz-Odendaal TA. 2016. The sclerotic ring of squamates: an evo-devo-eco perspective. *J Anat.* 229:1–11.

Badenhorst D, Hillier LDW, Literman R, Montiel EE. I, Radhakrishnan S, Shen Y, Minx P, Janes DE, Warren WC, Edwards SV, et al. 2015. Physical mapping and refinement of the painted turtle genome (*Chrysemys picta*) inform amniote genome evolution and challenge turtle-bird chromosomal conservation. *Genome Biol Evol.* 7:2038–2050.

Beatty DD. 1984. Visual pigments and the labile scotopic visual system of fish. *Vision Res.* 24:1563–1573.

Bellingham J, Chaurasia SS, Melyan Z, Liu C, Cameron MA, Tarttelin EE, Iuvone PM, Hankins MW, Tosini G, Lucas RJ. 2006. Evolution of melanopsin photoreceptors: discovery and characterization of a new melanopsin in nonmammalian vertebrates. *PLoS Biol.* 4:1334–1343.

Benoit J, Abdala F, Manger PR, Rubidge BS. 2016. The sixth sense in mammalians forerunners: variability of the parietal foramen and the evolution of the pineal eye in South African Permo-Triassic eutheriodont therapsids. *Acta Palaeontol Pol.* 61:777–789.

Bowmaker JK. 2008. Evolution of vertebrate visual pigments. *Vision Res.* 48:2022–2041.

Chiari Y, Cahais V, Galtier N, Delsuc F. 2012. Phylogenomic analyses support the position of turtles as the sister group of birds and crocodiles (Archosauria). *BMC Biol.* 10:65.

Crawford NG, Parham JF, Sellas AB, Faircloth BC, Glenn TC, Papenfuss TJ, Henderson JB, Hansen MH, Simison WB. 2015. A phylogenomic analysis of turtles. *Mol Phylogenet Evol.* 83:250–257.

Davies WIL, Collin SP, Hunt DM. 2012. Molecular ecology and adaptation of visual photopigments in craniates. *Mol Ecol.* 21:3121–3158.

Eakin RM. 1973. The Third Eye. 1st ed. Berkeley and Los Angeles (CA): University of California Press.

Edgar RC. 2004. MUSCLE: multiple sequence alignment with high accuracy and high throughput. *Nucleic Acids Res.* 32:1792–1797.

Emerling CA, Huynh HT, Nguyen MA, Meredith RW, Springer MS. 2015. Spectral shifts of mammalian ultraviolet-sensitive pigments (short wavelength-sensitive opsin 1) are associated with eye length and photic niche evolution. *Proc R Soc B* 282:20151817.

Enright JM, Toomey MB, Sato SY, Temple SE, Allen JR, Fujiwara R, Kramlinger VM, Nagy LD, Johnson KM, Xiao Y, et al. 2015. *Cyp27c1* red-shifts the spectral sensitivity of photoreceptors by converting Vitamin A1 into A2. *Curr Biol.* 25:3048–3057.

Ezcurra MD, Butler RJ. 2015. Taxonomy of the proterosuchid archosauriforms (Diapsida: Archosauromorpha) from the earliest Triassic of South Africa, and implications for the early archosauriform radiation. *Palaeontology* 58:141–170.

Falcón J, Besseau L, Fuentès M, Sauzet S, Magnanou E, Boeuf G. 2009. Structural and functional evolution of the pineal melatonin system in vertebrates. *Ann N Y Acad Sci.* 1163:101–111.

Fernández-Sampedro MA, Invergo BM, Ramon E, Bertranpetit J, Garriga P. 2016. Functional role of positively selected amino acid substitutions in mammalian rhodopsin evolution. *Sci Rep.* 6:21570.

Firth BT, Kennaway DJ. 1980. Plasma melatonin levels in the scincid lizard *Trachydosaurus rugosus*. *J Exp Biol.* 85:311–321.

Frigato E, Vallone D, Bertolucci C, Foulkes NS. 2006. Isolation and characterization of melanopsin and pinopsin expression within photoreceptive sites of reptiles. *Naturwissenschaften* 93:379–385.

Gerkema MP, Davies WIL, Foster RG, Menaker M, Hut RA. 2013. The nocturnal bottleneck and the evolution of activity patterns in mammals. *Proc R Soc B* 280:20130508.

Govardovskii VI, Chkheidze NI, Zueva LV. 1988. Morphofunctional investigation of the retina in the crocodilian caiman *Caiman crocodilus*. *Sensory Syst.* 1:19–25.

Green RE, Braun EL, Armstrong J, Earl D, Nguyen N, Hickey G, Vandewege MW, John JAS, Capella-gutiérrez S, Castoe TA, et al. 2014. Three crocodilian genomes reveal ancestral patterns of evolution among archosaurs. *Science* 346:1335.

Gundy GC, Ralph CL. 1975. Parietal eyes in lizards: zoogeographical correlates. *Science* 190:671–673.

Hankins MW, Peirson SN, Foster RG. 2008. Melanopsin: an exciting photopigment. *Trends Neurosci.* 31:27–36.

Hauser FE, Hazel IV, Chang BSW. 2014. Spectral tuning in vertebrate short wavelength-sensitive 1 (SWS1) visual pigments: can

wavelength sensitivity be inferred from sequence data? *J Exp Zool Part B Mol Dev Evol*. 322:529–539.
Hutchison VH, Kosh RJ. 1974. Thermoregulatory function of the parietal eye in the lizard *Anolis carolinensis*. *Oecologia* 16:173–177.
Joyce WG, Gauthier JA. 2004. Palaeoecology of triassic stem turtles sheds new light on turtle origins. *Proc Biol Sci*. 271:1–5.
Kappers JA. 1965. Survey of the innervation of the epiphysis cerebri and the accessory pineal organs of vertebrates. *Prog Brain Res*. 10:87–153.
Kato T, Jr, Todo T, Ayaki H, Ishizaki K, Morita T, Mitra S, Ikenaga M. 1994. Cloning of a marsupial DNA photolyase gene and the lack of related nucleotide sequences in placental mammals. *Nucleic Acids Res*. 22:4119–4124.
Kawano-Yamashita E, Koyanagi M, Terakita A. 2014. The evolution and diversity of pineal and parapineal photopigments. In: Hunt DM, Hankins MW, Collin SP, Marshall NJ, editors. Evolution of visual and non-visual pigments. New York, NY: Springer. p. 1–21.
Kearse M, Moir R, Wilson A, Stones-Havas S, Cheung M, Sturrock S, Buxton S, Cooper A, Markowitz S, Duran C, et al. 2012. Geneious Basic: an integrated and extendable desktop software platform for the organization and analysis of sequence data. *Bioinformatics* 28:1647–1649.
Lee MSY. 2013. Turtle origins: Insights from phylogenetic retrofitting and molecular scaffolds. *J Evol Biol*. 26:2729–2738.
Legendre LJ, Guénard G, Botha-brink J, Cubo J. 2016. Palaeohistological evidence for ancestral high metabolic rate in archosaurs. *Soc Syst Biol*. 65:989–996.
Levenson DH, Eckert SA, Crognale MA, Deegan JF, Jacobs GH. 2004. Photopic spectral sensitivity of green and loggerhead sea turtles. *Copeia* 2004:908–914.
Levenson DH, Ponganis PJ, Crognale MA, Deegan JF, Dizon A, Jacobs GH. 2006. Visual pigments of marine carnivores: Pinnipeds, polar bear, and sea otter. *J Comp Physiol A Neuroethol Sens Neural Behav Physiol*. 192:833–843.
Li C, Wu X-C, Rieppel O, Wang L-T, Zhao L-J. 2008. An ancestral turtle from the Late Triassic of southwestern China. *Nature* 456:497–501.
Liebman PA, Granda AM. 1971. Microspectrophotometric measurements of visual pigments in two species of turtle *Pseudemys scripta* and *Chelonia mydas*. *Vision Res*. 11:105–114.
Liu Y, Zhou Q, Wang Y, Luo L, Yang J, Yang L, Liu M, Li Y, Qian T, Zheng Y, et al. 2015. *Gekko japonicus* genome reveals evolution of adhesive toe pads and tail regeneration. *Nat Commun*. 6:1–11.
Loew ER, Govardovskii VI. 2001. Photoreceptors and visual pigments in the red-eared turtle, *Trachemys scripta elegans*. *Vis Neurosci*. 18:753–757.
Lyson TR, Rubidge BS, Scheyer TM, Smith RMH, Botha-brink J, Bever GS, Lyson TR, Rubidge BS, Scheyer TM, Queiroz KD, et al. 2016. Fossorial origin of the turtle shell. *Curr Biol*. 26:8–1.
Ma J, Znoiko S, Othersen KL, Ryan JC, Das J, Isayama T, Kono M, Oprian DD, Corson DW, Cornwall MC, et al. 2001. A visual pigment expressed in both rod and cone photoreceptors. *Neuron* 32:451–461.
Meredith RW, Gatesy J, Emerling CA, York VM, Springer MS. 2013. Rod monochromacy and the coevolution of cetacean retinal opsins. *PLoS Genet*. 9:e1003432.
Meredith RW, Gatesy J, Murphy WJ, Ryder OA, Springer MS. 2009. Molecular decay of the tooth gene Enamelin (*ENAM*) mirrors the loss of enamel in the fossil record of placental mammals. *PLoS Genet*. 5:e1000634.
Nagloo N, Collin SP, Hemmi JM, Hart NS. 2016. Spatial resolving power and spectral sensitivity of the saltwater crocodile, *Crocodylus porosus*, and the freshwater crocodile, *Crocodylus johnstoni*. *J Exp Biol*. 219:1394–1404.
Nesbitt SJ. 2011. The early evolution of archosaurs: Relationships and the origin of major clades. *Bull Am Museum Nat Hist*. 352:1–292.
Nesbitt SJ, Flynn JJ, Pritchard AC, Parrish JM, Ranivoharimanana L, Wyss AR. 2015. Postcranial osteology of *Azendohsaurus madagaskarensis* (?Middle to Upper Triassic, Isalo Group, Madagascar) and its systematic position among stem archosaur reptiles. *Bull Am Museum Nat Hist*. 398:1–126.
Nesbitt SJ, Turner AH, Weinbaum JC. 2013. A survey of skeletal elements in the orbit of Pseudosuchia and the origin of the crocodylian palpebral. *Earth Environ Sci Trans R Soc Edinb*. 103:365–381.
Niemiller ML, Fitzpatrick BM, Shah P, Schmitz L, Near TJ. 2013. Evidence for repeated loss of selective constraint in rhodopsin of amblyopsid cavefishes (Teleostei: Amblyopsidae). *Evolution* 67:732–748.
Phillips JA, Harlow HJ. 1981. Elevation of upper voluntary temperatures after shielding the parietal eye of horned lizards (*Phrynosoma douglassi*). *Herpetologica* 37:199–205.
Oaks JR. 2011. A time-calibrated species tree of Crocodylia reveals a recent radiation of the true crocodiles. *Evolution* 65:3285–3297.
Ohtsuka T. 1985. Spectral sensitivities of seven morphological types of photoreceptors in the retina of the turtle, *Geoclemys reevesii*. *J Comp Neurol*. 237:145–154.
Ohuchi H, Yamashita T, Tomonari S, Fujita-Yanagibayashi S, Sakai K, Noji S, Shichida Y. 2012. A non-mammalian type opsin 5 functions dually in the photoreceptive and non-photoreceptive organs of birds. *PLoS One* 7:e31534.
Okano T, Takanaka Y, Nakamura A, Hirunagi K, Adachi A, Ebihara S, Fukada Y. 1997. Immunocytochemical identification of pinopsin in pineal glands of chicken and pigeon. *Mol Brain Res*. 50:190–196.
Osborn AR, Almabruk KH, Holzwarth G, Asamizu S, LaDu J, Kean KM, Karplus PA, Tanguay RL, Bakalinsky AT, Mahmud T. 2015. De novo synthesis of a sunscreen compound in vertebrates. *Elife* 4:1–15.
Pignatelli V, Champ C, Marshall J, Vorobyev M. 2010. Double cones are used for colour discrimination in the reef fish, *Rhinecanthus aculeatus*. *Biol Lett*. 6:537–539.
Putnam NH, Connell BO, Stites JC, Rice BJ, Hartley PD, Sugnet CW, Haussler D, Rokhsar DS. 2016. Chromosome-scale shotgun assembly using an in vitro method for long-range linkage. *Genome Res*. 26:342–350.
Roth JJ, Gern WA, Roth EC, Ralph CL, Jacobson E. 1980. Nonpineal melatonin in the alligator (*Alligator mississippiensis*). *Science* 210:548–550.
Scheyer TM, Sander PM. 2007. Shell bone histology indicates terrestrial palaeoecology of basal turtles. *Proc Biol Sci*. 274:1885–1893.
Schoch RR, Sues H-D. 2015. A Middle Triassic stem-turtle and the evolution of the turtle body plan. *Nature* 523:584–587.
Schott RK, Müller J, Yang CGY, Bhattacharyya N, Chan N, Xu M, Morrow JM, Ghenu A-H, Loew ER, Tropepe V, et al. 2015. Evolutionary transformation of rod photoreceptors in the all-cone retina of a diurnal garter snake. *Proc Natl Acad Sci U S A*. 113:356–361.
Shedlock AM, Edwards SV. 2009. Amniotes (Amniota). In: Hedges SB, Kumar S, editors. The timetree of life. Oxford, UK: Oxford University Press. p. 375–379.
Sillman AJ, Ronan SJ, Loew ER. 1991. Histology and microspectrophotometry of the photoreceptors of a crocodilian, *Alligator mississippiensis*. *Proc R Soc B Biol Sci*. 243:93–98.
Simões BF, Sampaio FL, Douglas RH, Casewell NR, Harrison RA, Nathan S, Partridge JC, Hunt DM, Gower DJ. 2016. Visual pigments, ocular filters and the evolution of snake vision. *Mol Biol Evol*. 33:2483–2495.
Simões BF, Sampaio FL, Loew ER, Sanders KL, Fisher RN, Hart NS, Hunt DM, Partridge JC, Gower DJ. 2016. Multiple rod—cone and cone—rod photoreceptor transmutations in snakes: evidence from visual opsin gene expression. *Proc R Soc B Biol Sci*. 283:20152624.
Stamatakis A. 2014. RAxML version 8: a tool for phylogenetic analysis and post-analysis of large phylogenies. *Bioinformatics* 30:1312–1313.
Stebbins RC, Eakin RM. 1958. The role of the third eye in reptilian behavior. *Am Mus Novit*. 1958:1–40.
Su C-Y, Luo D-G, Terakita A, Shichida Y, Liao H-W, Kazmi MA, Sakmar TP, Yau K-W. 2006. Parietal-eye phototransduction components and their potential evolutionary implications. *Science* 311:1617–1621.
Tomonari S, Migita K, Takagi A, Noji S, Ohuchi H. 2008. Expression patterns of the opsin 5-related genes in the developing chicken retina. *Dev Dyn*. 237:1910–1922.
Wada S, Kawano-Yamashita E, Koyanagi M, Terakita A. 2012. Expression of UV-sensitive parapinopsin in the iguana parietal eyes and its

implication in UV-sensitivity in vertebrate pineal-related organs. *PLoS One* 7:e39003.
Walls G. 1942. The vertebrate eye and its adaptive radiation. London, UK: Hafner Publishing Company.
Wan Q-H, Pan S-K, Hu L, Zhu Y, Xu P-W, Xia J-Q, Chen H, He G-Y, He J, Ni X-W, et al. 2013. Genome analysis and signature discovery for diving and sensory properties of the endangered Chinese alligator. *Cell Res*. 23:1091–1105.
Wang Z, Pascual-Anaya J, Zadissa A, Li W, Niimura Y, Huang Z, Li C, White S, Xiong Z, Fang D, et al. 2013. The draft genomes of soft-shell turtle and green sea turtle yield insights into the development and evolution of the turtle-specific body plan. *Nat Genet*. 45:701–706.
Witherington B, Bjorndal KA. 1991. Influence of wavelength and intensity on hatchling sea turtle phototaxis: implications for sea-finding behavior. *Copeia* 4:1060–1069.
Yang Z. 2007. PAML 4: Phylogenetic analysis by maximum likelihood. *Mol Biol Evol*. 24:1586–1591.
Yokoyama S. 2008. Evolution of dim-light and color vision pigments. *Annu Rev Genomics Hum Genet*. 9:259–282. 2.